

Photocatalytic Fuel Cell Incorporated With Persulphate Activation for Electricity Production by Diluted Palm Oil Mill Effluent Treatment

Sze-Mun Lam^{1,2}, Jin-Chung Sin^{1,2}, Honghu Zeng²

¹Faculty of Engineering and Green Technology, Universiti Tunku Abdul Rahman, 31900 Kampar, Perak, Malaysia
lamsm@utar.edu.my

²College of Environmental Science and Engineering, Guilin University of Technology, Guilin 541004, China
zenghonghu@glut.edu.cn

Abstract - In this study, a new and effective photocatalytic fuel cell incorporated with peroxydisulfate activation (PDS/PFC) system was devised to treat diluted palm oil mill effluent (POME) and electricity production. This designed system contained ZnO nanorod array (NRA)/Zn photoanode and copper oxide/Cu cathode. Compared to the PDS/photocatalytic (PC) activation and PFC alone, the PDS/PFC system revealed exceptional performance. Using 0.5 mM PDS, the PDS/PFC system exhibited the remarkable chemical oxygen demand (COD) removal efficiency of 78.4% and maximum power density (P_{max}) of 6.981 mW cm⁻². The boosted photoelectrocatalytic activity can be attributed to the addition of PDS to extend the active species reactions from the interface of electrodes to the whole POME solution. Moreover, the PDS can serve as an effective electron acceptor to suppress the charge carrier recombination. The best PDS concentration was also scrutinized in the developed PDS/PFC system. The radical scavenging tests were also carried out to testify the existence of active species in the mineralization reaction. The comprehensive photoelectrocatalytic mechanism was finally elucidated.

Keywords: ZnO Anode, Oxidant, Photocatalytic fuel cell, Palm oil mill effluent

1. Introduction

The use of fossil fuel massively raised the carbon dioxide emission in the world and consequently led to environmental deterioration. A fuel cell is an effective system in recuperating chemical energy into electrical energy. Among the fuel cell, photocatalytic fuel cell deems as is a superlative technology that can recycle energy, while removing the contaminants [1,2]. In the PFC system, an electron-hole pair in the anode photocatalyst was photoexcited under the light irradiation. The hole oxidized and eliminated the contaminants, while the electron formed in the anode shunted to the cathode, yielding electricity [3]. For this reason, the performance of PFC relied on the photoanode capability to initiate the photoelectrocatalytic reaction.

In recent decades, TiO₂ and ZnO photocatalysts have been extensively applied due to their chemical stabilities, ease of availabilities, low cost and strong photo-oxidizing abilities. In some reports [4], ZnO can harvest a larger light spectrum range than TiO₂. In particular, the one-dimensional (1D) ZnO nanorods structures made electron-hole transfer easier because of their larger surface areas. The major lapse of the ZnO photoanode was the drawback of the rapid electron-hole recombination and limited surface area that can confine the mass transport and redox reactions [5,6]. Researchers have explored the myriad ways to enhance the photoanode material for facilitate electron-hole transfer in treating contaminants and power generation.

It was worth noting that peroxydisulfate (PDS) has been broadly exploited as an adaptable in-situ oxidant and low cost in wastewater remediation [8,9]. Upon the activation, PDS can produce sulfate radicals (SO₄•⁻) which could intensify the redox reactions from the electrode surface to the entire PFC system. Additionally, the PDS could be served as an electron acceptor to boost the electron-hole segregation on the photoanode, accelerating the active radical species production and electron transfer [10]. Inspired by above consideration, a collaborative system by placing PDS into PFC (PDS/PFC) to treat diluted palm oil mill effluent (POME) and electricity generation concomitantly. This combined system contained ZnO nanorod arrays (NRA)/Zn photoanode and CuO/Cu cathode. Meanwhile, the POME was chosen as a typical wastewater in this study as the palm oil is a very important commodity in Malaysia and their direct discharge into the water bodies can cause severe pollution to the receiving water system. At last, the POME treatment mechanism was also carried out using radical scavenging experiments to explicate the function of numerous active species in the photoelectrocatalytic processes.

2. Experimental

2.1. Synthesis of ZnO/Zn NRA Photoanode

A Zn foil with dimension 15.0 cm x 2.0 cm was first ultrasonically cleaned using ethanol and distilled water. Then, a ZnO seed solution was prepared by mixing 20 mM of zinc acetate with 10 mM of sodium hydroxide in 50 mL ethanol solution. Afterwards, the ZnO seed solution was heated at 100 °C for 1 hour under stirring, the ZnO seed solution was casted onto the Zn plate and calcined in a furnace at 300 °C for 1 h. The casting of ZnO seed solution was at least coated onto the Zn plate for 2 layers. Meanwhile, the synthesis of CuO/Cu cathode was revealed in our earlier report [6].

2.2. Characterization

The film-typed sample was characterized by a X-ray diffractometer (XRD, Philips PW1820) and field-emission scanning electron microscope (FESEM, JEOL 6701-F).

2.3. Evaluation of Photoelectric and Photocatalytic Tests

The typical PFC setup was developed by an anodic ZnO/Zn NRA and cathodic CuO/Cu in a 100 mL of POME solution. Air was provided closed to the CuO/Cu cathode via an air pump at 2 L min⁻¹. The two electrodes were linked via an external circuit with a resistivity of 1 kΩ. The test solution was constantly mixed with the aid of a magnetic stirrer during the reaction. Prior to the experiment, the PFC system was placed in the dark for 30 min. The system was then carried out under a UV-C light irradiation. The measured average light intensity was 5400 mW cm⁻² by a radiometer. The distance between the anodic and cathodic materials were set at 4 cm. Chemical oxygen demand (COD) removal of POME solution was measured using a UV-vis spectrophotometer. The current-voltage characteristic of PFC system was monitored by a multimeter. The power density was computed using the equation, P (mW cm⁻²) = JV , where J and V are the current density in mA cm⁻² and voltage in mV, respectively.

3. Results and Discussion

3.1. Material Characterization

Surface morphology of the ZnO NRA/Zn photoanode is illustrated in Fig. 1a. It can be seen that the ZnO NRA/Zn photoanode presented well-ordered and densely arranged 1D structure with an average diameter of around 280 nm. This structure resulted in oriented electron transport from ZnO NRA surface to Zn, which can enable the electron-hole pairs segregation in photoelectrocatalytic processes [2]. The crystal phase of the ZnO NRA/Zn photoanode surface depicted in Fig. 1b indicated that the ZnO NRA layer has a wurtzite ZnO (JCPDS file 36-1451). The enhanced photocatalytic performance of ZnO comprised wurtzite phase has been demonstrated in literature reports [5,6].

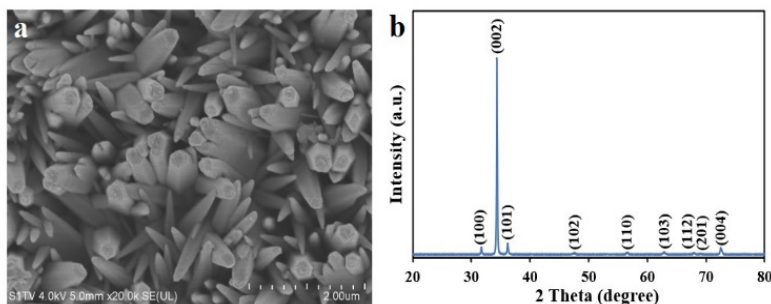


Fig. 1. FESEM image (a) and XRD spectrum (b) of the ZnO NRA/Zn photoanode surface.

3.2. Enhanced POME Treatment using PDS/PFC System

The efficiencies of different PDS-added approaches, namely photocatalysis (PDS/PC) and photocatalytic fuel cell (PDS/PFC) on the COD removal of POME were evaluated. As shown in Fig. 2a, the COD removal of POME was 28.7% and 39.6% by the PC and PFC alone after 240 min UV light irradiation in the absence of PDS oxidant, respectively. Nonetheless, when the PDS oxidant was added, the COD efficiencies of the PC and PFC were improved to 51.2% and 78.4%, respectively. The COD removal reached only 21.9% when the PC or PFC system under photolysis condition (data not

shown). This outcome indicated a synergistic function for POME treatment occurred after PDS integrated to PFC and the synergistic effect of the PDS/PFC was superior to the PDS/PC.

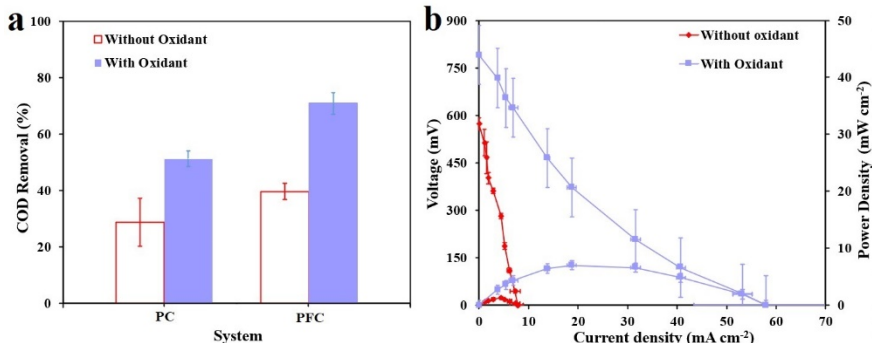


Fig. 2. (a) COD removal of POME by 0.5 mM PDS oxidant intergrated with PC and ZnO NRA/Zn PFC approaches, and (b) polarization (*I-V*) and power density (*P-V*) plots of PFC and PDS/PFC systems.

Fig. 2b depicts a polarization (*I-V*) and and power density (*P-V*) plots associated with the PFC and PDS/PFC systems were compared. The maximum power density (P_{max}) and short-circuit current (J_{SC}) values of PFC improved after the incorporation of PDS. The P_{max} of the PDS/PFC was about 6.981 mW cm^{-2} , which was approximately 5.6 times higher than that of the PFC alone. By adding PDS, the open-circuit voltage (V_{OC}) and J_{SC} values improved from 573 mV and 7.8 mA cm^{-2} to 790.5 mV to 57.9 mA cm^{-2} , respectively. The photoelectric findings of the PDS/PFC system in comparison to the PFC alone was because of the mutual effect of activation of PDS and accelerated electron transfer for the photoelectrocatalytic process under exposure of UV light.

The effect of oxidant concentration on the POME treatment in the PDS/PFC was scrutinized by adjusting the concentrations of oxidant from 0.25 to 2.5 mM. As indicated in Fig. 3a, the POME mineralization process increased when elevating the PDS concentrations. The COD removal efficiency at the concentration of 0.25 mM PDS after 240 min attained 39.6%. As the PDS concentration was enhanced to 2.5 mM, the COD removal efficiency improved to 88.9%. In the PDS/PFC system, the activation of PDS could produce the additional sulphate anion radicals ($SO_4^{\bullet-}$), which can boost the photoelectrocatalytic reaction between active species and POME pollutants on the interface of photoelectrodes-electrolyte [7-9]. Thence, increasing the PDS would be resulted more active radicals participated in the mineralization of POME and power output of the PFC system.

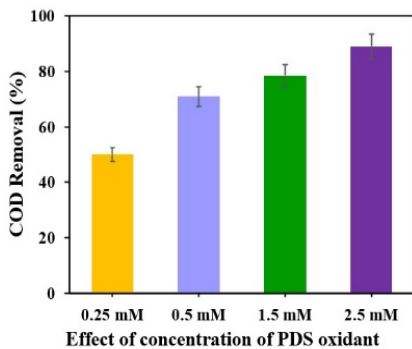


Fig. 3. Effect of PDS oxidant concentration on POME treatment in PDS/PFC system.

In order to testify the contribution of active species in the mineralization process of the PDS/PFC system, radical scavenger tests were carried out with 1,4-benzoquinone (1,4-BQ), ethylenediaminetetraacetic acid disodium salt (EDTA-2Na), ethanol, tertiary butanol (t-butanol) and silver nitrate ($AgNO_3$) being selected to specifically quench superoxide anion radical ($O_2^{\bullet-}$), hole (h^+), $SO_4^{\bullet-}$, hydroxyl radical ($\bullet OH$), and electron (e^-), respectively. As exhibited in Fig. 4a, 88.9% of COD was removed when no scavenging agent was added. Nevertheless, the POME treatment was tremendously inhibited with the

addition of ethanol and *t*-butanol, which were merely 19.8% and 31.9%, respectively. Meanwhile, the COD removal efficiencies were observed in the presence of EDTA-2Na, silver nitrate and BQ were merely 46.3%, 51.4% and 57.4%, respectively. These data manifested that $\text{SO}_4^{\bullet-}$ and $\bullet\text{OH}$ were the two pivotal active species that influenced the photoelectrocatalytic performance of the developed PFC system, while h^+ , $\text{O}_2^{\bullet-}$ and e^- exhibited a marginal but positive contribution to the POME treatment.

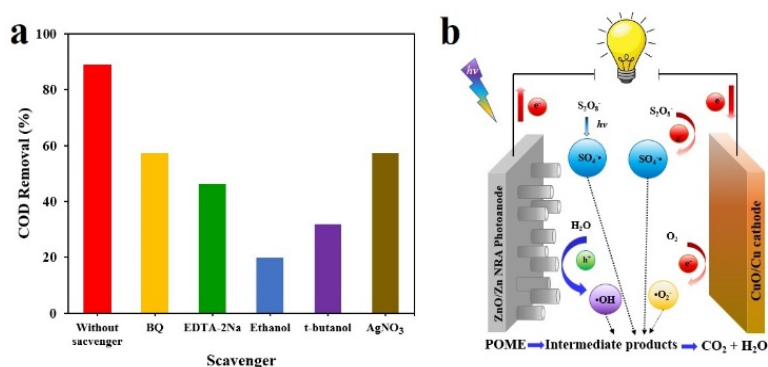


Fig. 4. (a) Contribution of different oxidants on POME treatment by PDS/PFC system, and (b) The possible working principle of the proposed PDS/PFC system composed of ZnO NRA photoanode.

Based on the radical scavenging tests, a tentative mechanism for the POME treatment in the PDS/PFC system was proposed (Fig. 4b). Upon the UV irradiation, the ZnO NRA on the Zn film underwent photoexcitation and e^- will be transferred from valence band (VB) to conduction band (CB) and left the h^+ in the VB. The h^+ in VB of ZnO will react with water molecule to form $\bullet\text{OH}$ radicals and participated in POME decomposition. Meanwhile, the e^- will be shunted to the cathode via external circuit and underwent the reduction reaction with the surrounded dissolved oxygen. In the presence of PDS oxidant, the e^- can also reduce the $\text{SO}_4^{\bullet-}$ from the dissociation of PDS and extended the active species reactions from the surface of electrodes to the whole POME solution. Additionally, the $\text{SO}_4^{\bullet-}$ could be generated through UV light activation of the PDS [10]. In this way, the PDS/PFC system allowed the efficient segregation of charge carriers in both electrodes and eventually yielded the $\text{SO}_4^{\bullet-}$ and $\bullet\text{OH}$ active species for destruction of POME [11-13]. It was also noteworthy to highlight that the 1-D ZnO NRA with short diffusion length can provide the effective charge carrier segregation ability. Ergo, in presence of PDS oxidant, 1-D ZnO NRA PFC can endow the remarkable POME treatment and concomitantly generated the electricity.

4. Conclusion

In summary, a PFC incorporated with a PDS activation was utilized for the diluted POME treatment and concomitant with production of electricity. Compared to the PDS/PC activation and PFC alone, the PDS/PFC system demonstrated outstanding photoelectrocatalytic activity. Using 0.5 mM PDS, the PDS/PFC system exhibited the remarkable COD removal efficiency of 78.4% and P_{max} of 6.981 mW cm^{-2} . Integration of PDS in the PFC system prolonged the active species reactions from the interface of electrodes to the whole POME solution. At the same time, the PDS can also serve as an effective electron acceptor to quench the charge carrier recombination. The best PDS concentration was also determined in the developed PDS/PFC system. Moreover, the radical scavenging tests validated that $\text{SO}_4^{\bullet-}$ and $\bullet\text{OH}$ acted as core active species in the POME mineralization. Thence, the PDS/PFC system enabled an effective approach to collect clean energy from real wastewater treatment.

Acknowledgements

This research was supported by Ministry of Higher Education of Malaysia (MoHE) through Fundamental Research Grant Scheme (FRGS/1/2022/TK0/UTAR/02/5 and FRGS/1/2019/TK02/UTAR/02/4), Guangxi Key Laboratory of Theory and Technology for Environmental Pollution Control (1801K012 and 1801K013), ASEAN Talented Young Scientist Program of Guangxi (DT2200002995), special funding for Guangxi “Bagui Scholar” construction project, and L'Oréal-UNESCO Research Grant.

References

- [1] Q. O. Sun, S. H. Wu, D. You, T. Zang, L. F. Dong, “Novel composite functional photocatalytic fuel cell assisted by Fenton-like reactions,” *Appl. Surf. Sci.*, vol. 467–468, pp. 825–835, 2019.
- [2] M. W. Kee, J. W. Soo, S. M. Lam, J. C. Sin, A. R. Mohamed, “Evaluation of photocatalytic fuel cell (PFC) for electricity production and simultaneous degradation of methyl green in synthetic and real greywater effluents,” *J. Environ. Manage.*, vol. 228, pp. 383–392, 2018.
- [3] K. A. Wong, S. M. Lam, J. C. Sin, “Wet chemically synthesized ZnO structures for photodegradation of pre-treated palm oil mill effluent and antibacterial activity,” *Ceram. Intern.*, vol. 45, pp. 1868–1880, 2019.
- [4] S. M. Lam, J.C. Sin, A. Z. Abdullah, A. R. Mohamed, “Degradation of wastewaters containing organic dyes photocatalysed by zinc oxide: a review,” *Desalin. Water Treat.*, vol. 41, pp. 131–169, 2012.
- [5] K. P. Yuan, Q. Cao, X. Y. Li, H. Y. Chen, Y. H. Deng, Y. Y. Wang, W. Luo, H. L. Lu, D. W. Zhang, “Synthesis of $\text{WO}_3@Zn\text{WO}_4@ZnO\text{-ZnO}$ hierarchical nanocactus arrays for efficient photoelectrochemical water splitting,” *Nano Energy*, vol. 41, pp. 543–551, 2017.
- [6] J. C. Sin, C. A. Lim, S. M. Lam, A. R. Mohamed, H. H. Zeng, “Facile synthesis of novel ZnO/Nd-doped BiOBr composites with boosted visible light photocatalytic degradation of phenol,” *Mater. Lett.*, vol. 248, pp. 20–23, 2019.
- [7] B. Weng, S. Q. Liu, Z. R. Tang, Y. J. Xu, “One-dimensional nanostructure based materials for versatile photocatalytic applications,” *RSC Adv.*, vol. 4, pp. 12685-12700, 2014.
- [8] J. C. Sin, C. A. Lim, S. M. Lam, A. R. Mohamed, H. H. Zeng, “Facile synthesis of novel ZnO/Nd-doped BiOBr composites with boosted visible light photocatalytic degradation of phenol,” *Mater. Lett.*, vol. 248, pp. 20–23, 2019.
- [9] H. Katsumata, Y. Oda, S. Kaneco, S. Tohru, “Photocatalytic activity of Ag/CuO/ WO_3 under visible-light irradiation,” *RSC Adv.*, vol. 3, pp. 5028–5035, 2013.
- [10] K. Li, H. Zhang, T. Tang, Y. Xu, D. Ying, Y. Wang, J. Jia, “Optimization and application of $\text{TiO}_2/\text{Ti-Pt}$ photo fuel cell (PFC) to effectively generate electricity and degrade organic pollutants simultaneously,” *Water Res.* vol. 62, pp. 1–10, 2014.
- [11] W. Liu, M. L. Wang, C. X. Xu, S. F. Chen, X. L. Fu, “ $\text{Ag}_3\text{PO}_4/\text{ZnO}$: An efficient visible-light-sensitized composite with its application in photocatalytic degradation of Rhodamine B,” *Mater. Res. Bull.*, vol. 48, pp. 106–113, 2013.
- [12] W. Liu, M. L. Wang, C. X. Xu, S. F. Chen, X. L. Fu, “Significantly enhanced visible-light photocatalytic activity of g- C_3N_4 via ZnO modification and the mechanism study,” *J. Mol. Catal. A: Chem.*, vol. 368–369, pp. 9–15, 2013.
- [13] H. Katsumata, Y. Oda, S. Kaneco, S. Tohru. “Photocatalytic activity of Ag/CuO/ WO_3 under visible-light irradiation,” *RSC Adv.*, vol. 3, pp. 5028–5035, 2013.
- [14] Q. Zeng, J. Bai, J. Li, L. Li, L. Xia, B. Zhou, Y. Sun, “Highly-stable and efficient photocatalytic fuel cell based on an epitaxial $\text{TiO}_2/\text{WO}_3/\text{W}$ nanothorn photoanode and enhanced radical reactions for simultaneous electricity production and wastewater treatment,” *Appl. Energy*, vol. 220, pp. 127–137, 2018.
- [15] J. L. Tang, Y. H. Pu, X. C. C. Wang, Y. S. Hu, J. Huang, H. H. Ngo, S. W. Pan, Y. Y. Li, N. M. Zhu, “Effect of additional food waste slurry generated by mesophilic acidogenic fermentation on nutrient removal and sludge properties during wastewater treatment,” *Bioresour. Technol.*, vol. 294, pp.122218, 2019.
- [16] APHA, “Standard Methods for the Examination of Water and Wastewater”, twenty-first Ed. American Public Health Association, Washington DC, USA, 2005.